Desalination and Water Treatment
www.deswater.com
doi: 10.5004/dwt.2023.29829

308 (2023) 217–228
October

Application of the central composite design and response surface methodology for optimization of reactive color removal from aqueous solutions using dicyandiamide-formaldehyde resin modified by ammonium chloride

Hamid Karyab, Zahra Hamidi, Fatemeh Ghotbinia, Zohre Mosa Khani, Niloofar Nazeri*

Social Determinants of Health Research Center, Qazvin University of Medical Sciences, Bahonar Boulevard, Qazvin 34197-59811, Iran, Tel.: +98 28 33344838; Fax: +98 28 33344839; emails: n.nazeri@qums.ac.ir (N. Nazeri), hkaryab@gmail.com (H. Karyab), zahraahamidi75@gmail.com (Z. Hamidi), qotbiff@gmail.com (F. Ghotbinia), zoh.mohammad@gmail.com (Z. Mosa Khani)

Received 17 December 2022; Accepted 1 August 2023

ABSTRACT

This analysis was extended to optimize the elimination of three mixed reactive colors including yellow 145, red 195, and blue 19 from wastewater using dicyandiamide-formaldehyde (DCD-F) resin. The synthesis of resin was conducted in controlled conditions and Fourier-transform infrared spectroscopy was performed to identify the nature of the synthesized resin structure. The investigation strategy, formulated on the response surface methodology (RSM) by the central composite design (CCD), was applied to optimize the impacts of the three operating factors of the coagulation and flocculation processes together with contact time (30–60 min), pH (5–9), and DCD-F dosage (0.5–1.5 mg/L) on the response, which was color removal (%). In addition, several linear and non-linear kinetic and isotherm models and thermodynamic parameters were used to assess the capacity and behavior of adsorption processes and dye mass transfer on DCD-F resin surface. Using RSM/CCD, the optimized conditions of contact time, pH, and polymer dosage were found to be 30 min, 7.18, and 1.3 mg/L, respectively. Assessing the linear and non-linear kinetic and isotherm models indicated that the dyes adsorption on DCD-F resin was fitted with linear pseudo-second-order type II and non-linear Freundlich models, respectively. In the best fitted isotherm model, the adsorption capacity was 726.3 mg/g and the kinetic study revealed that the adsorption process of reactive dyes on polymer is due to physicochemical interactions between the two phases of DCD-F resin and solute. In addition, the thermodynamic results including entropy, enthalpy and Gibbs free energy disclosed that the adsorption of reactive dyes on the synthesized resin was likely to be influenced by a physisorption mechanism. The results also disclosed that the resin can efficiently eliminate the reactive dye over an extended pH range. Therefore, it can be concluded that the DCD-F resin as an effective flocculant can be used to eliminate reactive dyes from colored wastewater in optimized conditions.

Keywords: Reactive dye; Wastewater; Dicyandiamide resin; Response surface methodology

1. Introduction

The textile industry is the largest water-consuming industries in the world that produce a high volume of wastewater. Wastewater encompasses substantial dyes, organic and inorganic contents for-instance heavy metals (Cu, As, Cr, and Zn) [1], and is one of the most important environmental pollutants [2] due to its toxicity and carcinogenicity [3,4]. Dyes utilized in the textile industry are resistant to biodegradation due to their high molecular weight

* Corresponding author.

and complicated structures. Direct discharge of this sewage into the treatment plant causes disruption and shock to the biological system of the treatment plant [5]. Dyes are generally categorized into three groups: comprising anionic (direct, acidic, and reactive), cationic (basic), and non-ionic (dispersed) dyes. The anionic group is the most widely used dyes globally [1,6]. In recent years, reactive dyes have been widely used due to better processing, the wide variety of their color spectrum, and the increased use of cotton fibers. Reactive dyes react and stabilize the fibers under the influence of heat and alkaline solution [3]. Dye removal techniques from textile industrial wastewater are divided into three clusters such as biological, physical, and chemical methods [7,8]. Biological techniques include the use of microorganisms and enzymes. Physical techniques include membrane filtration and irradiation. Chemical techniques include the use of oxygenated water, sodium hypochlorite, ozone, the use of photocatalysts, electrolysis, and advanced oxidation methods [4]. In addition, in numerous studies, the usage of nanomaterials including nano-adsorbent Mn-doped CuO-nanoparticles loaded on activated carbon, and graphene oxide/sodium montmorillonite nanocomposite were successfully reported [9,10]. Among all the dye removal techniques, the coagulation–flocculation process is among the most prominent, cost-effective, and is a highly efficient methods in wastewater treatment [11,12]. The basis of coagulation and flocculation of reactive dyes is the destabilization of stable colloids (particles with a size of 1 nm–1 μm) that possess a surface negative charge. The coagulant, by neutralizing the charge of the colloids, destabilizes them and causes them to settle [5]. Iron and aluminum salts are the highly prevalent mineral coagulants. Although the use of these coagulants leads to the removal of the dye, the formed clots are light and need more time to settle. Therefore, they are not efficient enough to remove dyes from colored wastewater. In addition, the use of these coagulants can cause equipment corrosion and their high level of Al^{3+} can cause secondary pollution of the effluent. In recent years, special emphasis has been laid on the use of synthetic organic polymers as coagulants with improved flocculation properties. Polymeric coagulants, by virtue of their sizeable molecules and the formation of long and heavy chains between the coagulant and the dye molecules, have improved the dye removal performance [13–15]. The mechanism of synthetic polymeric coagulants is based on neutralizing the charge of the colloidal particles and bridging them by contracting the thickness of the electrical double layer. The advantage of polymeric coagulants over mineral coagulants is that they create more stable flocs formation and increase the sedimentation rate [14,16]. Dicyandiamide-formaldehyde (DCD-F) resin is a kind of positively charged coagulant that is used in wastewater treatment [14,17]. The addition of the cationic polymer of DCD-F to the effluent neutralizes the negative charge of the colloidal particles which ultimately leads to flocs formation, sedimentation, and consequently the removal of large amounts of color, turbidity, and suspended solids [18,19]. Most dye removal studies focus on conventional methods, that evaluate the color removal as the result of changing one parameter and maintaining other parameters at a steady level [19]. This method is time consuming and prevents it from reaching the optimum conditions because the interactions between the variables are not considered. Via RSM, the design technique can overcome these limitations [20] and achieve optimal results through the assessment of multiple parameters. The technique reduces the number of experiments, development time and consequently overall costs [21–23]. It has been implemented to investigate the simultaneous outcome of different variables such as pH, dye concentration, coagulation dose, and settling time for assessing the performance of the efficacy of polymer coagulants in the removal of dyes [1]. Based on the best knowledge of the authors, although DCD-F has been used broadly as a coagulant/flocculant for the removal of dye pollution from water in different studies, there are no reports on the investigation of the optimum condition for maximum removal of anionic dyes by synthesized resin. Thus, in this research, we focused on synthesizing the DCD-F resin as a decolorizing agent and evaluating the simultaneous effects of the operating parameters in the coagulation and flocculation processes including pH, sedimentation time (min), and DCD-F dosage (mg/L) on the color removal efficiency (%) implementing the central composite design (CCD) and RSM. The Box–Behnken experimental design model was used for precisely determine the role of individual process parameters, the interactions among the variables, and to optimize the process variables.

2. Materials and methods

2.1. Materials

Dicyandiamide with a solubility of 2.26%@13°C, formaldehyde solution (37%), and ammonium chloride were supplied by Sigma-Aldrich (USA). NaOH, H_2SO_4, NaCl, and Na_2CO_3 were purchased from Merck (Germany). Reactive yellow 145 ($C_{28}H_{20}ClN_9Na_4O_{16}S5$) (MW: 1026.3; solubility in water: 80 g/L at 20°C), reactive blue 19 ($C_{22}H_{16}N2Na_2O_{11}S_3$) (MW: 626.5; solubility in water: 220 g/L at 20°C) and reactive red 195 ($C_{31}H_{24}ClN_7Na_5O_{19}S_6$) (MW: 1141.4; solubility in water: 100 g/L at 20°C) were obtained from Alvan Company (Iran).

2.2. Synthesis of DCD-F resin and characterization

To synthesize the DCD-F resin, formaldehyde solution (37%) and dicyandiamide were poured in sequence into a 250 mL three-necked flask, and the pH was adjusted below 2 by adding hydrochloric acid (30%). The mixture was heated at reflux for 2 h in an oil bath at 70°C–80°C, then ammonium chloride was appended to the flask and the mixture was agitated for 1 h more. The molar ratio of formaldehyde: dicyandiamide: ammonium chloride within the mixture was 3:1:0.7 [3,24,25]. Finally, the product was chilled to ambient temperature. Fourier-transform infrared (FTIR) spectra of DCD-F resin were conducted with an FTIR spectroscopy (EQUINOX55, Bruker Optics, Ettlingen, Germany) to evaluate and identify the nature of the synthesized DCD/F resin.

2.3. Experimental procedure

The synthesized wastewater was prepared by imitating the operating conditions of the textile industry for the three reactive dyes: blue, yellow, and red. For this purpose,

2 g of each dye, 3.2 g of NaOH, 2 g of NaCl, and 3.2 g of Na_2CO_3 were disintegrated in 20 L of water and warmed at 50°C for 1 h to completely hydrolyze [3]. The prepared sample was stored at ambient air until the analysis was done. After that, a six-beaker jar-test equipment was utilized to optimize the color removal procedure from the synthesized wastewater in the coagulation and flocculation processes. In running the jar test, 1 L of synthesized wastewater was poured into each vessel and its pH was adjusted with 2N H_2SO_4 and 1N NaOH in the range 5–9. Then, rapid mixing was carried out for 1 min at 200 rpm, followed by tentative agitation defined as 10 min at 50 rpm [3]. In this experiment, the mixing time (min) and the velocity (rpm) in coagulation and flocculation were kept constant. These values were optimized in previous studies. Thus, after the pre-test, the optimized parameters were used according to the experimental plan [26,27]. After sedimentation at the experimental range (30–60 min), the supernatant was removed for the color measurement. The dye removal from the samples was measured by the ADMI method following the conventional approaches for examining water and wastewater [28], using UV-Vis HACH spectrophotometer DR/6000 at a wavelength equivalent to the maximum absorbance from 400 to 700 nm. Finally, the dye removal from the aqueous solutions was calculated utilizing Eq. (1). In this equation, C_r and C_t are the color concentrations in the raw and treated wastewater, correspondingly.

$$\text{Color removal}(\%) = \frac{(C_r - C_t)}{C_r} \quad (1)$$

2.4. Experimental design and data analysis

The process parameters, namely contact time (*A*), DCD-F resin dosage (*B*), and pH (*C*) were optimized by RSM. The association uniting the aforementioned variables and the pertinent feedback was characterized by a central composite design using Design–Expert-12 software during the experimental period. CCD is the most popular class of second-order designs useful in response surface methodology. It is well suited for building and fitting a quadratic model for the response variable without the need to use a complete three-level factorial experiment [29,30]. As presented in Table 1, the examined range of the contact time in the sedimentation process was 30–60 min, while the range of DCD-F resin concentration was 0.5–1.5 mg/L, and the range of pH was adjusted from 5 to 9. As presented in Table 2, the sum total of experiments was 20 along with 8 factorial points, 6 axial points, and 6 replicate points corresponding with CCD [31]. The best-fit model can be presumed after the quadratic model analysis by analysis of variance and *F*-value determination as shown in Eq. (2); where *Y* is the color removal % as a response; *n* the number of variables; x_i and x_j the coded values of the factors; and b_0, b_i, b_{ii}, and b_{ij} are the constant coefficient, the linear coefficient, the quadratic coefficient, and the interaction coefficient, respectively. The affiliation amid the features and the predicted outcome was approximated using the proceeding second-order polynomial model [31].

$$Y = b_o + \sum_{i=1}^{n} b_i x_i + \sum_{i=1}^{n} b_{ii} x_i^2 + \sum_{i=1}^{n-1} \sum_{j=i+1}^{n} b_{ij} x_i x_j \quad (2)$$

2.5. Isotherm and kinetic studies

Equilibrium linear and non-linear isotherm models were used to assess the capacity of dye adsorption on the

Table 2
Experimental design and observed responses of the central composite design

Run order	Variables			Response (%)
	X_1	X_2	X_3	
1	45	0.16	7	9.89
2	45	1	7	89.16
3	30	0.5	5	14.15
4	30	0.5	9	9.60
5	60	1.5	9	91.50
6	45	1	3.60	92.70
7	60	0.5	5	18.75
8	70.1	1	7	85.62
9	45	1	7	83.33
10	45	1	7	92.39
11	30	1.5	9	92.6
12	60	0.5	9	9.61
13	45	1	10.36	45.00
14	45	1	7	86.87
15	45	1.84	7	95.93
16	45	1	7	87.08
17	19.77	1	7	87.50
18	45	1	7	86.40
19	30	1.5	5	94.89
20	60	1.5	5	94.89

Table 1
Independent variables in actual and coded levels in central composite design

Independent variables				Range and levels (coded)				
Factors	Coded	Symbol	Unit	Low (–1)	Central (0)	High (1)	–α	+α
Contact time	X_1	*A*	min	30	45	60	19.77	70.23
Coagulant	X_2	*B*	mg/L	0.5	1	1.5	0.16	1.84
pH	X_3	*C*	–	5	7	9	3.64	10.36
Response			%					

polymer surface. All experiments were conducted under optimized conditions of 1,130 mg/L of DCD-F resin and a pH of 7.0. The capacity and rate of color adsorption by DCD-F resin surface were also assessed at dye concentrations of 100, 200, 300, 400 and 500 mg/L with a coagulation, flocculation and sedimentation time of 1, 10 and 30 min, respectively. In addition, the mixing velocity was set 200 and 50 rpm during the coagulation and flocculation process. After experimental tests, five isotherms, including Langmuir and Freundlich, as two-parameter isotherms, and Temkin, as three-parameter isotherms, were employed to describe the equilibrium adsorption of reactive dyes on DCD-F resin surface [32,33]. The coefficient of R^2 values were used to describe the adsorption process. Linear expressions and appropriate plots to predict the reactive dyes adsorption performance are provided in Table 3. In addition, to conduct the non-linear isotherm experiments, the initial dye concentrations (C_o) of dicyandiamide surface were used. After reaching equilibrium, the equilibrium concentrations (C_e) were determined and the adsorption capacity at equilibrium (q_e) was calculated for each concentration. The appropriate graphs were plotted for each model. Finally, the non-linear adsorption parameters were determined using Graph Pad Prism software (Version 8.0) by plotting q_e (g/mg) vs. C_e (mg/L). Marquardt's percent standard deviation (MPSD) and hybrid fractional error function (HYBRID) were used to properly assess the fit of the isotherms. The equations for MPSD and HYBRID are as follows; where q_i^{Exp} and q_i^{Cal} are the experimental and calculated adsorbed color by CS nanoparticles [Eqs. (3) and (4)]. P is the number of parameters in the regression model and N is the number of observations in the experimental isotherm.

$$\mathrm{MPSD} = 100\sqrt{\left(\frac{1}{N-P}\sum_{i=1}^{N}\left(\frac{q_i^{\mathrm{Exp}}-q_i^{\mathrm{Cal}}}{q_i^{\mathrm{Exp}}}\right)^2\right)} \tag{3}$$

$$\mathrm{HYBRID} = \frac{100}{N-P}\sum_{i=1}^{N}\left[\frac{\left(q_i^{\mathrm{Exp}}-q_i^{\mathrm{Cal}}\right)^2}{q_i^{\mathrm{Exp}}}\right] \tag{4}$$

Five linear and non-linear kinetic models including the pseudo-first-order and pseudo-second-order kinetic type I, type II, type III, and type IV were used to assess the adsorption process of dyes on the DCD-F resin surface (Table 4). All batch experiments were performed under optimized

Table 3
Linear and non-linear isotherm models in the reactive dyes' adsorption on DCD-F resin surface

Isotherms	Non-linear expression	Linear expression	Plot	Parameters
Freundlich	$q_e = K_F(C_e)^{1/n}$	$\ln q_e = \ln K_F + n^{-1}\ln C_e$	$\ln q_e$ *vs.* $\ln C_e$	K_F = exp(intercept) n = (slope)$^{-1}$
Langmuir	$q_e = (q_m K_L C_e)/(1 + K_L C_e)$	Type I: $C_e/q_e = (1/K_L q_m) + (C_e/q_m)$	(C_e/q_e) *vs.* C_e	q_m = (slope)$^{-1}$ K_L = slope/intercept
		Type II: $1/q_e = (1/K_L q_m C_e) + (1/q_m)$	$1/q_e$ vs. $1/C_e$	q_m = (intercept)$^{-1}$ K_L = intercept/slope
		Type III: $q_e = q_m - (1/K_L)q_e/C_e$	q_e vs. q_e/C_e	q_m = intercept K_L = −(slope)$^{-1}$
		Type IV: $q_e/C_e = K_L q_m - K_L q_e$	q_e/C_e vs. q_e	q_m = −(intercept/slope) K_L = −slope
Temkin	$q_e = q_m \ln(K_T C_e)$	$q_e = q_m \ln K_T + q_m \ln C_e$	q_e vs. $\ln C_e$	q_m = slope K_T = exp(intercept/slope)

Table 4
Used kinetic models and their linear and non-linear form in the adsorption of reactive dyes on DCD-F resin surface

Kinetic models		Linear	Non-linear	Plot	Parameters
Pseudo-first-order		$\ln(q_e - q_t) = \ln q_e - k_{1p}t$	$q_t = q_e(1-e^{-k_1 t})$	$\ln(q_e - q_t)$ vs. t	q_e = exp(intercept) k_{1p} = −(slope)
Pseudo-second-order	Type I	$t/q_t = 1/k_{2p}q_e^2 + t/q_e$	$q_t = (q_e^2 k_2 t)/(1 + q_e k_2 t)$	t/q_t vs. t	q_e = slope^{-1} k_{2p} = (slope^2)/intercept
	Type II	$1/q_t = (1/k_{2p}q_e^2)(1/t) + (1/q_e)$		$1/q_t$ vs. $1/t$	q_e = intercept^{-1} k_{2p} = (intercept^2)/slope
	Type III	$q_t = q_e - (1/k_{2p}q_e)q_t/t$		q_t vs. q_t/t	q_e = intercept k_{2p} = −1/(slope × intercept)
	Type IV	$q_t/t = k_{2p}q_e^2 - k_{2p}q_e q_t$		q_t vs. q_t	q_e = −intercept/slope k_{2p} = (slope^2)/intercept

conditions of 1,130 mg/L of DCD-F resin and pH equal to 7.1 at room temperature (21°C ± 3°C) and 3 levels including 5, 15, and 25 min. In addition, error functions including the normalized standard deviation (NSD) and average relative error (ARE) were applied to select the optimum kinetic model using Eqs. (5) and (6) [32,33].

$$\mathrm{NSD} = 100\sqrt{\left(\frac{1}{N-1}\sum_{i=1}^{N}\left[\frac{q_t^{\mathrm{Exp}} - q_t^{\mathrm{Cal}}}{q_t^{\mathrm{Exp}}}\right]_i^2\right)} \tag{5}$$

$$\mathrm{ARE} = \frac{100}{N}\sum_{i=1}^{N}\left|\frac{q_i^{\mathrm{Exp}} - q_i^{\mathrm{Cal}}}{q_i^{\mathrm{Exp}}}\right| \tag{6}$$

In addition, the pH at the point of zero charge (pH_{PZC}) of the adsorbent was measured by adding 20 mL of 0.050 M NaCl to several Erlenmeyer flasks. A range of initial pH values (pH_i) of the NaCl solutions was adjusted from 2 to 10 by adding either 0.1 M of NaOH and HCl. The total volume of the solution in each flask was brought to precisely 30 mL by further addition of 0.05 M NaCl solution. The pH_i values of the solutions were then measured and noted and 30.0 mg of DCD-F resin was added to each flask, which were capped immediately. The suspensions were shaken in a shaker at 25°C and allowed to equilibrate for 48 h. The suspensions were then centrifuged at 3600 rpm for 10 min. The final pH was measured and plotted against the initial pH. The pH at which the curve intersected was taken as pH_{PZC}. The adsorbent net surface charge is an effective parameter for its ion exchange properties.

2.6. Thermodynamic adsorption experiments

The thermodynamic parameters such as Gibbs free energy ($\Delta G°$), the entropy change ($\Delta S°$) and the enthalpy change ($\Delta H°$) during the adsorption were used to study the dyes' adsorption mechanism on DCD-F resin. For this purpose, 300 mg/L reactive dye solutions were adsorbed by 1,130 mg/L of DCD-F resin at three temperatures of 15°C, 30°C, and 45°C and pH 7.1. After the adsorption process, the remaining dye concentration was detected and the equilibrium adsorption amount was calculated. The entropy, enthalpy and Gibbs free energy at each temperature were calculated using Van't Hoff's equation. According to Van't Hoff equation, equilibrium constant for adsorption (K_c) at each temperature was calculated from Eq. (7), where q_e and C_e are the adsorption capacity at equilibrium (mg/g) and equilibrium concentration (mg/L), respectively. The free energy change ($\Delta G°$) at each temperature was determined by using Eq. (8). In addition, in order to determine $\Delta H°$ and $\Delta S°$, a straight line of $\ln K_c$ vs. $1/T$ was plotted to calculate the $\Delta H°$ and $\Delta S°$ from the slope ($-\Delta H°/R$) and the intercept ($\Delta S°/R$) of the plot, respectively [18,34].

$$K_C = \frac{q_e}{C_e} \tag{7}$$

$$\Delta G° = -RT\ln\left(K_C\right) \tag{8}$$

3. Results and discussion

3.1. Characterization of the synthesized DCD-F resin

Fig. 1 shows the FTIR spectra of the synthesized DCD-F resin. The absorption peaks around 1,540 and 1,630 cm^{-1} emanated from a carbonyl of the unreacted formaldehyde, and the absorption peaks around 3,100 and 3,300 cm^{-1} were caused by the stretching vibration of –NH– and $–NH_2$, respectively. Accordingly, the amino groups can be protonated, provide a positive charge in the polymer structure and improve the decolorization. It should be noted that the peak of C≡N stretching vibration, which is related to the native structure of DCD was not found at about 2,390 cm^{-1} [35,36].

3.2. Fitting of the quadratic model

The experiments were performed under the conditions determined by RSM. The quadratic model was chosen based on the statistical outcomes of the recommended model which is summarized in Table 5.

Table 6 provides information associated with the analysis of variance for the response level of the suggested

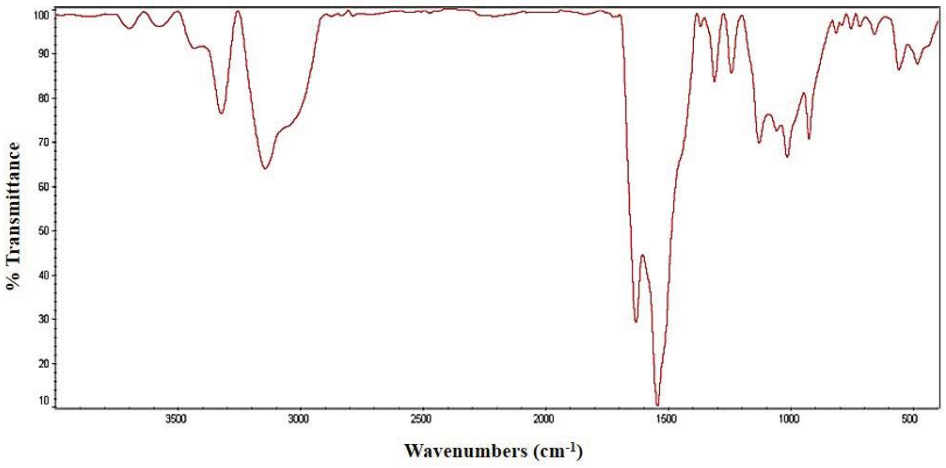

Fig. 1. Fourier-transform infrared spectra of the synthesized DCD-F resin.

quadratic model. The probability of the *F*-value (269.69) implied that the suggested model was significant for optimizing color removal from the dye wastewater using DCD-F resin, while the error function was insignificant. Statistical analyses revealed that the adjusted R^2 (0.99) was consistent with the predicted R^2 (0.98), and the variance was less than 0.2. The value of the Prob. > *F* was less than 0.05, whereas the lack of fit was insignificant.

Subsequently, an empirical full quadratic model equation regarding the 3 independent variables was developed for the color removal % (Eq.9). Optimization of the model parameters was attained by specifying the importance of each variable to reach the maximum color removal from an aqueous solution. According to Table 6 and by using quadratic regression, the base-coded relationship between response and all variables can be described by Eq. (9).

$$\begin{aligned}\text{Color removal}(\%) = {} & +88.09 + 0.29A + 34.42B - 7.03C \\ & - 0.26AB - 0.26AC + 1.45BC \\ & - 3.4A^2 - 15.16B^2 - 9.72C^2 \end{aligned} \quad (9)$$

3.3. Interaction effects of dosage and sedimentation time with pH variation

Fig. 2 shows the interactive influence of coagulant concentration and sedimentation time on the color removal efficacy at different pH values. All the diagrams illustrate that at different pH values (pH 5, 7, 9), the color removal efficacy increased as the concentration of coagulant increased. According to Fig. 2c, it is obvious that, with the increase of the coagulant concentration up to 1.1 mg/L at any time point, the color removal increased to 100%, and the addition of coagulant concentration up to 1.5 mg/L could not induce any change in the color removal. This can be interpreted based on the premise that the upsurge in coagulant concentration, increased the number of reaction sites available to start the reaction between the polymer and dye molecules to form flocs. That is, an elevation in the coagulant concentration may result in more surface collisions with more dye molecules to enhance dye entrapment [37]. As the free dye molecules reduced, increasing the coagulant concentration did not change the color removal like the previous, and the rate of color removal decreased. The effect of the pH variation on the color removal revealed that the maximum color removal can be achieved at a pH of 7 and any change in pH value can reduce the efficacy. This is consistent with Joo et al.'s [3] finding, which demonstrated that the dye removal efficiency was highly reliant on the pH value. In another study, the effect of pH on the reactive dye removal was assessed by measuring the zeta charge. It was reported that the zeta charge decreased with increasing pH from 3 to 7.5, while it declined slightly below a pH of 7.5 [38]. However, a different result was reported by Wang et al. [17]. They assessed the color removal from the aqueous dye solutions by the DCD-F polymer modified with ammonium chloride in the

Table 5
Model summery statistics

Source	Std. Dev.	R^2	Adjusted R^2	Predicted R^2	PRESS	Lack of fit
Linear	21.05	0.6763	0.6069	0.4406	10,722.58	<0.0001
2FI	23.72	0.6772	0.5012	–0.5891	30,462.84	<0.0001
Quadratic	2.81	0.9967	0.9930	0.9812	360.26	0.6068

Table 6
Analysis of variance for response surface quadratic model in removal of color by DCD-F coagulant

Source	Sum of squares	df	Mean square	*F*-value	*p*-value	
Model	19,106.37	9	2,122.93	269.69	<0.0001	Significant
A-Time	1.14	1	1.14	0.1443	0.7140	
B-Dosage	14,285.42	1	14,285.42	1,814.78	<0.0001	
C-pH	42.18	1	42.18	5.36	0.0493	
AB	0.5513	1	0.5513	0.0700	0.7980	
AC	0.5408	1	0.5408	0.0687	0.7999	
BC	16.88	1	16.88	2.14	0.1813	
A^2	0.4010	1	0.4010	0.0509	0.8271	
B^2	3,219.87	1	3,219.87	409.04	<0.0001	
C^2	1,340.89	1	1,340.89	170.34	<0.0001	
Residual	62.97	8	7.87			
Lack of fit	18.03	3	6.01	0.6685	0.6068	Not significant
Pure error	44.95	5	8.99			
Adjusted R^2	0.9930					
Predicted R^2	0.9812					

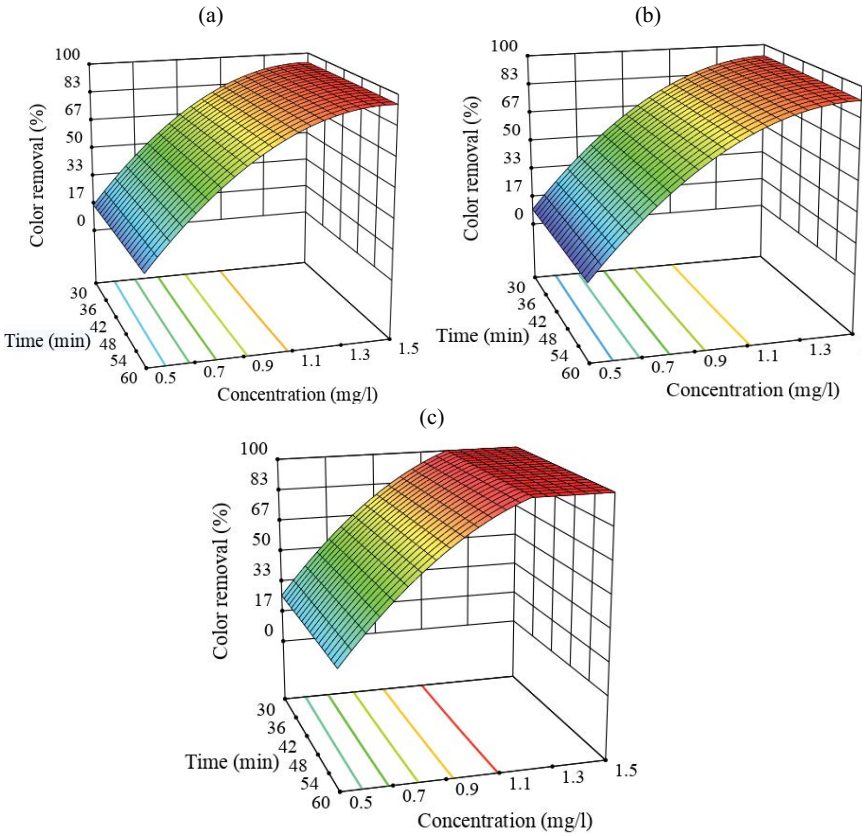

Fig. 2. Response surface graphs for color removal efficiency with interactions between contact time (min) and DCD-F dosage in different pH ranges; (a) pH = 5, (b) pH = 9, and (c) pH = 7.

pH range of 6.8–7.8. They concluded that the pH variation had no significant modification on the color removal.

3.4. Interaction effects of dosage and pH with sedimentation time variation

Different studies have examined the consequence of sedimentation time on the color removal efficacy and reported different contact times (30–60 min) as optimum conditions because they were affected by different variables like dye concentration, coagulant concentration, pH, and temperature [39,40]. As presented in Fig. 3, the interaction effects of pH and coagulant dosage were examined, and the optimized condition showed that neutral solutions had higher efficiency in color removal during sedimentation operation than acidic and alkaline conditions. The results revealed that the sedimentation of flocs lasted less than 30 min and the size of flocs was heavy enough to settle down. In addition, it was revealed that the increasing contact time from 30 min to 60 min did not change the efficiency of floc removal in the settling unit. One of the limitations of the present study was that the maximum color removal from wastewater was achieved at a minimally assessed retention time in the sedimentation unit. Besides, the selected range of retention time in the sedimentation was based on previous studies and experiments [17,35,38]. Therefore, we suggest that a lower retention time for color removal by DCD-F resin should be assessed in future studies.

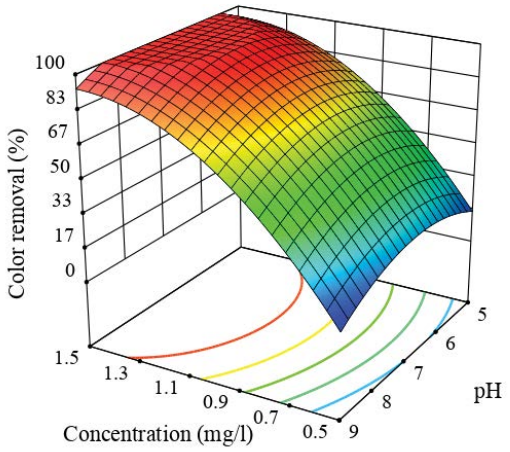

Fig. 3. Response surface graphs for color removal with interaction between DCD-F dosage and pH in contact time of 30 min.

The pH_{PZC} of adsorbents specifies the chemical potential of the functional groups of the surfaces. The pH_{PZC} of the DCD-F was found to be 8 (Fig. 4). This result actually suggests that when the pH of the solution < pH_{PZC}, the adsorbent is positively charged and there is an electrostatic attraction between negatively charged reactive dyes and positively charged adsorbent [10].

3.5. Interaction effects of pH and sedimentation time with polymer dosage variation

Fig. 5 depicts that DCD-F dosage has a dominant effect on color removal efficiency, which confirmed previous findings by Joo et al. [3] who reported that dye removal efficiency increased as polymer dosage increased. The diagram shows that neutral, unlike acidic and alkaline solutions, have a higher color removal propensity. In other words, the higher response area is found at the top of the convex while the response decreases through the navigation of the curve from neutral pH to the alkaline and acidic zones. pH can affect the color removal and determine the coagulation efficiency because the distribution form and solubility of the decolorizers and dyes are remarkably influenced by pH. The coagulant exhibited maximum color removal (100%) at neutral pH when compared to alkaline (84%) or acidic (86%) conditions. As the row water recycling plant inflow became neutral (or close to neutral), it can be concluded that no further adjustment of the pH was required to increase color removal [35]. This effect can be explained by the fact that the DCD-F coagulant is a positively charged polymer that is easily soluble in a neutral solution and can react with soluble dyes to form a precipitate [13]. On the other hand, in aqueous solutions, the synthetic reactive dye can dissolve, and its sulfonate group dissociates and converts to anionic dye ions which are ready to react with positive functional groups on the DCD-F coagulant [41]:

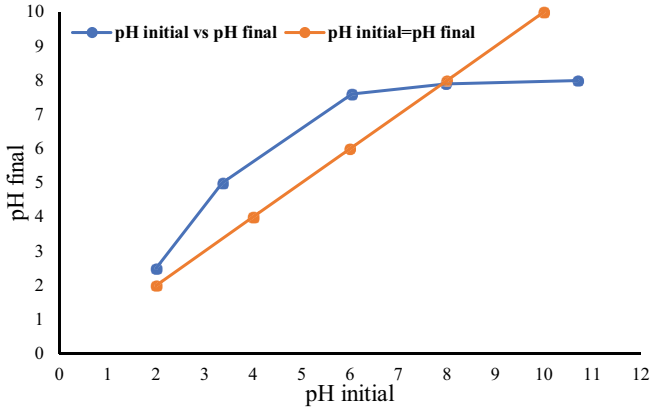

Fig. 4. Determination of the pH of point of zero charge (pH_{ZPC}) of DCD-F resin.

$$DSO_3Na + H_2O \rightarrow DSO^{-3} + Na^+$$

Nevertheless, at a high pH, the resin amine group may deprotonate, leading to an increased electrostatic repulsion between the dye molecules and the resin, and ultimately reducing the number of dye molecules bound to the resin [42]. A similar scenario may be repeated at low pH, such that the sulfonate group of the dye molecules cannot dissociate, and the anionic reaction sites are not formed to react with

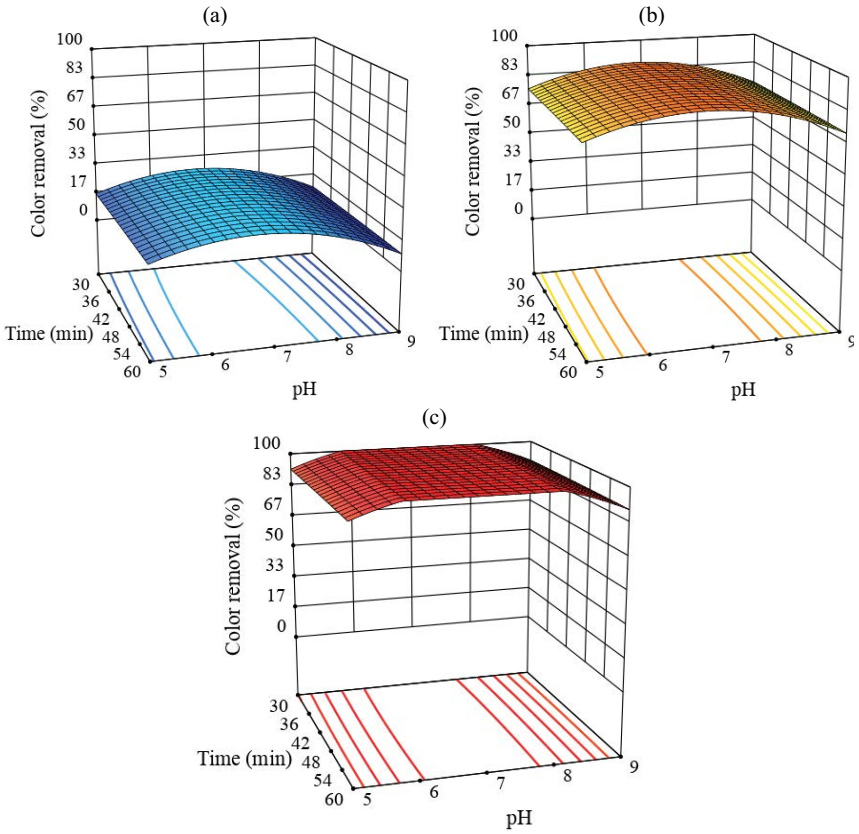

Fig. 5. Response surface graphs for color removal efficiency with interactions between sedimentation time (min) and pH: (a) dosage 0.5 mg/L, (b) dosage 0.8 mg/L, and (c) dosage 1.3 mg/L.

the positively charged resin. These verdicts were consistent with previous reports [43].

However, as illustrated in Fig. 5, by augmenting coagulant dosage, the color removal efficiency increased to more than 80% in all pH ranges. It can be observed that polymer bridging had a major impact on the color removal at alkaline or acidic pH, while charge neutralization contributed mainly to the color removal at pH 7 [43]. A similar outcome was reported by other researchers, who recorded the highest color removal efficiency (for Reactive Blue 19 (RB19)) at pH 7 [44]. Table 7 illustrates the optimized conditions of reactive dye removal from wastewater in different studies.

3.6. Isotherm, kinetic, and thermodynamic adsorption studies

Table 8 shows the isotherm parameters obtained by using the linear and non-linear fitting analysis. However, the non-linear isotherm models had higher R^2 values compared to the linear forms, and the calculated error values were lower in linear isotherm models. In terms of correlation coefficient and error values, assessing linear and non-linear models indicated that the dye adsorption on DCD-F resin was fitted with non-linear Freundlich model with an adsorption capacity (q_m) of 726.3 mg/g. It indicates that the adsorbent surface is heterogeneous, and the functional sites have exponential distribution [46–48]. Although the correlation coefficient of Freundlich was equal to that of Temkin's model (R^2 = 0.989), the results showed that the non-linearized Freundlich isotherm significantly reduced the adsorption prediction error. The Freundlich model has been widely applied to describe the adsorption of chemicals using different adsorbents. In this isotherm K_F, which represents the relative adsorption intensity of the adsorbent with respect to the bonding energy, was obtained 726.3 mg/g, indicating a good intensity of reactive dyes on DCD-F resin surface. In addition, n is the heterogeneity factor which indicates the deviation from linearity of adsorption. The n value depends on the adsorbent and solute characteristics and the heterogeneity of the adsorbent sites and $n > 2$ indicates an efficient adsorption. The calculated n value for the reactive dyes adsorption was 833.3 which is related to the high efficiency of DCD-F resin for reactive dyes adsorption [46–48].

The obtained results from the kinetic study using different linear and non-linear models (Table 9) indicate that the linear pseudo-second-order type II was the most suitable model to describe the adsorption process of color by DCD-F resin surface with the highest coefficients of determination (R^2 value of 0.997) and the lowest error functions

Table 7
Optimized conditions of reactive dye removal from wastewater in different studies

Coagulant	pH	Coagulant dosage	Sedimentation time (min)	Dye removal efficiency (%, experimental)	Dye removal efficiency (%, predicted)	References
Ferric chloride sludge	3.5	236.6 mg/L	–	96.5	100	[45]
DCD-F-ammonium chloride	6.8–7.8	0.1 mL/L	30	51.74	–	[17]
Melamine-F-ammonium chloride	6.8–7.8	0.1 mL/L	30	47.27	–	[17]
DCD-F	5	0.25 g/L	30	62	–	[3]
Poly(epichlorohydrin-dimethylamine)	6	0.15 g/L	20	96.4	–	[38]
DCD-F-ammonium chloride	7.1	1.13 mg/L	<30	70.5	100	Present study

Table 8
Isotherms parameters by linear and non-linear regression method for the reactive dyes adsorption on DCD-F resin surface

Linear isotherms	R^2	MPSD	HYBRID	Parameters
Freundlich	0.864	45.97	55.13	n = 5,000; K_F = 6.57 mg/g
Langmuir type I	0.656	56.41	58.46	K_L = 6.58 L/mg; q_m = 8.65 mg/g
Langmuir type II	0.891	50.23	37.03	K_L = 0.054 L/mg; q_m = 138.89 mg/g
Langmuir type III	0.898	54.34	54.74	K_L = 19.26 L/mg; q_m = 8.20 mg/g
Langmuir type IV	0.789	53.81	63.72	K_L = 0.35 L/mg; q_m = 8.72 mg/g
Temkin	0.864	362.97	17.28	K_T = 0.6.07 L/mg; q_m = 481.98 mg/g
Non-linear isotherms	R^2	MPSD	HYBRID	Parameters
Freundlich	0.989	18.57	38.6	n = 833.3; K_F = 726.3 mg/g
Langmuir type I	0.962	256.16	110,567.9	K_L = 0.001 L/mg; q_m = 1,000 mg/g
Langmuir type II	0.877	47.66	5,805.6	K_L = 6.20 L/mg; q_m = 0.05 mg/g
Langmuir type III	0.961	45.54	5,439.9	K_L = 256.41 L/mg; q_m = 8.29 mg/g
Langmuir type IV	0.975	59.68	8,440.2	K_L = 0.136 L/mg; q_m = 39.41 mg/g
Temkin	0.989	81.97	12,802.2	K_T = 0.007 L/mg; q_m = 40.93 mg/g

Table 9
Kinetic models parameters by linear regression method for the reactive dyes adsorption on dicyandiamide polymer surface

Linear models	R^2	NSD	ARE	Parameters
Pseudo-first-order	0.851	29.19	12.46	k_{1p} = 0.048 h^{-1}; q_m = 345.54 mg/g
Pseudo-second-order (Type I)	0.993	16.40	2.26	k_{2p} = 0.00005 mg/g·h; q_m = 2,000 mg/g
Pseudo-second-order (Type II)	0.997	15.18	2.83	k_{2p} = 0.000046 mg/g·h; q_m = 2,000 mg/g
Pseudo-second-order (Type III)	0.972	15.57	3.01	k_{2p} = 0.000045 mg/g·h; q_m = 1,979.1 mg/g
Pseudo-second-order (Type IV)	0.972	13.18	2.98	k_{2p} = 0.00019 mg/g·h; q_m = 2,005.42 mg/g
Non-linear models	R^2	NSD	ARE	Parameters
Pseudo-first-order	0.982	29.277	12.50	k_{1p} = 35.39 h^{-1}; q_m = 111.02 mg/g
Pseudo-second-order (Type I)	0.952	29.276	8.34	k_{2p} = 2.91 mg/g·h; q_m = 38.17 mg/g
Pseudo-second-order (Type II)	0.954	29.276	8.33	k_{2p} = 12.43 mg/g·h; q_m = 474.9 mg/g
Pseudo-second-order (Type III)	0.335	75.21	13.55	k_{2p} = 0.04 mg/g·h; q_m = 172.54 mg/g
Pseudo-second-order (Type IV)	0.902	33.73	9.59	k_{2p} = 0.474 mg/g·h; q_m = 51.50 mg/g

Table 10
Thermodynamic parameters of DCD-F resin on reactive dyes

Temperature (°C)	K_c	$\Delta G°$ (kJ/mol)	$\Delta H°$ (kJ/mol)	$\Delta S°$ (kJ/mol)
15	33.44	–8,331.78		
30	47.16	–9,708.00	8.3E-5	0.032
45	55.29	–10,603.23		

(NSD = 15.18 and ARE = 2.83). Kinetic models are normally used to consider the adsorption mechanism and the potential rate of the processes such as mass transfer and chemical reactions [49]. It was clearly shown that the experimental points of reactive dye adsorption on DCD-F resin conform to the pseudo-second-order model rather than the pseudo-first-order, followed by the linear pseudo-first-order model; therefore, the linear pseudo-second-order type II was selected to describe reactive dye adsorption on the resin surface. In the pseudo-second-order kinetic model, the rate-controlling phase is the surface adsorption of pollutants which involves chemisorption and the removal from a solution is due to physicochemical interactions between the two phases of solid and solute [50].

As shown in Table 10, the thermodynamic adsorption study showed that the enthalpies are greater than zero, thus the adsorption of reactive dyes is an endothermic process. The ionic motion in the solution is more intense with the increase of temperature, which is beneficial to the adsorption process. The positive values of entropies illustrate that the degree of disorder of the adsorbent surface increases during the adsorption process. However, the Gibbs free energy of DCD-F resin is less than zero and it can be concluded that the adsorption process can proceed spontaneously without requiring an input of energy from any external source [51,52].

4. Conclusion

The present study aimed to optimize the capability of DCD-F resin modified by ammonium chloride to remove three mixed reactive colors including Reactive Yellow 145, Reactive Blue 19 and Reactive Red 195 from solution. The obtained results revealed that the color removal efficiency was strongly influenced by the initial pH and coagulant dosage variations, and the optimum condition occurred at the coagulant dosage of 1.13 mg/L, and pH of 7.1. In addition, it was observed that the non-linear Freundlich isotherm model described the reactive dyes adsorption process, better than the Langmuir and Temkin isotherm models with the adsorption capacity of 726.3 mg/g. Also, assessing the linear and non-linear kinetic models reveals that the dyes adsorption on DCD-F resin was fitted with linear pseudo-second-order type II, indicating that the reactive dyes adsorption on polymer is due to physicochemical interactions between the two phases of resin and solute. Furthermore, the thermodynamic results including entropy, enthalpy and Gibbs free energy disclosed that the adsorption of reactive dyes on the resin is likely to be influenced by a physisorption mechanism. In summary, it can be concluded that the synthesized DCD-F resin modified with ammonium chloride, under the optimized conditions prepared in this study can be recommended as an appropriate coagulant in the removal of reactive color + from textile industry wastewater with neutral pH.

Acknowledgements

The authors acknowledge the Qazvin University of Medical Sciences for providing the technical and financial support.

Conflict of interest

The authors declare that they have no conflict of interest.

References

[1] I.A. Obiora-Okafo, O.D. Onukwuli, Optimization of coagulation-flocculation process for colour removal from azo dye using natural polymers: response surface methodological approach, Niger. J. Technol., 36 (2017) 482–495.
[2] M.A. Hassaan, A. El Nemr, Health and environmental impacts of dyes: mini review, Am. J. Environ. Sci. Eng., 1 (2017) 64–67.

[3] D.J. Joo, W.S. Shin, J.-H. Choi, S.J. Choi, M.-C. Kim, M.H. Han, T.W. Ha, Y.-H. Kim, Decolorization of reactive dyes using inorganic coagulants and synthetic polymer, Dyes Pigm., 73 (2007) 59–64.
[4] S. Mani, P. Chowdhary, R.N. Bharagava, Textile Wastewater Dyes: Toxicity Profile and Treatment Approaches, R. Bharagava, P. Chowdhary, Eds., Emerging and Eco-Friendly Approaches for Waste Management, Springer, Singapore, 2019. Available at: https://doi.org/10.1007/978-981-10-8669-4_11
[5] I.A. Obiora-Okafo, M.C. Menkiti, O.D. Onukwuli, Utilization of response surface methodology and factor design in micro-organic particles removal from brewery wastewater by coagulation/flocculation technique, Int. J. Appl. Sci. Math., 1 (2014) 15–21.
[6] K. Al-Zawahreh, M.T. Barral, Y. Al-Degs, R. Paradelo, Comparison of the sorption capacity of basic, acid, direct and reactive dyes by compost in batch conditions, J. Environ. Manage., 294 (2021) 113005, doi: 10.1016/j.jenvman.2021.113005.
[7] N. Rajesh Jesudoss Hynes, J. Senthil Kumar, H. Kamyab, J. Angela Jennifa Sujana, O.A. Al-Khashman, Y. Kuslu, A. Ene, B. Suresh Kumar, Modern enabling techniques and adsorbents-based dye removal with sustainability concerns in textile industrial sector-a comprehensive review, J. Cleaner Prod., 272 (2020) 122636, doi: 10.1016/j.jclepro.2020.122636.
[8] D. Bhatia, N.R. Sharma, J. Singh, R.S. Kanwar, Biological methods for textile dye removal from wastewater: a review, Crit. Rev. Env. Sci. Technol., 47 (2017) 1836–1876.
[9] E. Sharifpour, E. Alipanahpour Dil, A. Asfaram, M. Ghaedi, A. Goudarzi, Optimizing adsorptive removal of malachite green and methyl orange dyes from simulated wastewater by Mn-doped CuO-nanoparticles loaded on activated carbon using CCD-RSM: mechanism, regeneration, isotherm, kinetic, and thermodynamic studies, Appl. Organomet. Chem., 33 (2019) e4768, doi: 10.1002/aoc.4768.
[10] P. Arabkhani, A. Asfaram, M. Ateia, Easy-to-prepare graphene oxide/sodium montmorillonite polymer nanocomposite with enhanced adsorption performance, J. Water Process Eng., 38 (2020) 101651, doi: 10.1016/j.jwpe.2020.101651.
[11] B. Shi, G. Li, D. Wang, C. Feng, H. Tang, Removal of direct dyes by coagulation: the performance of preformed polymeric aluminum species, J. Hazard. Mater., 143 (2007) 567–574.
[12] S. Arslan, M. Eyvaz, E. Gürbulak, E. Yüksel, A Review of State-of-the-Art Technologies in Dye-Containing Wastewater Treatment – The Textile Industry Case, E. P.A. Kumbasar, A.E. Körlü, Eds., Textile Wastewater Treatment, InTechOpen, 2016.
[13] S.H. Lan, P. Ma, H.X. Lan, H. Zhang, X.W. Wu, Y.D. Wang, Study on the flocculation treatment of simulative dyeing wastewater by the dicyandiamide formaldehyde polymer, Appl. Mech. Mater., 522 (2014) 192–195.
[14] N.A. Oladoja, Headway on natural polymeric coagulants in water and wastewater treatment operations, J. Water Process Eng., 6 (2015) 174–192.
[15] H. Rong, B. Gao, R. Li, Y. Wang, Q. Yue, Q. Li, Effect of dose methods of a synthetic organic polymer and PFC on floc properties in dyeing wastewater coagulation process, Chem. Eng. J., 243 (2014) 169–175.
[16] E.K. Tetteh, S. Rathilal, Application of Organic Coagulants in Water and Wastewater Treatment, A. Sand, E. Zaki, Eds., Organic Polymers, InTechOpen, 2019.
[17] H. Zhang, H. Yang, J. Lu, Z. Wang, H. Gao, C. Liang, Y. Sun, Preparation, application, and mechanism of starch modified dicyandiamide formaldehyde polymer–bentonite microparticle retention and drainage aid system, BioResources, 14 (2019) 5883–5899.
[18] S. Uzunsakal, S. Zeytinci, Ö.L. Uyanık, N. Uyanık, Adsorption kinetics studies of polymeric nanocomposite coagulants, Polym. Polym. Compos., 21 (2013) 161–170.
[19] M. Khayet, A.Y. Zahrim, N. Hilal, Modelling and optimization of coagulation of highly concentrated industrial grade leather dye by response surface methodology, Chem. Eng. J., 167 (2011) 77–83.
[20] S. Ghafari, H.A. Aziz, M.H. Isa, A.A. Zinatizadeh, Application of response surface methodology (RSM) to optimize coagulation–flocculation treatment of leachate using poly-aluminum chloride (PAC) and alum, J. Hazard. Mater., 163 (2009) 650–656.
[21] N. Nazeri, M.R. Avadi, M.A. Faramarzi, S. Safarian, G. Tavoosidana, M.R. Khoshayand, A. Amani, Effect of preparation parameters on ultra-low molecular weight chitosan/hyaluronic acid nanoparticles, Int. J. Biol. Macromol., 62 (2013) 642–646.
[22] A. Barazandeh, H.A. Jamali, H. Karyab, Equilibrium and kinetic study of adsorption of diazinon from aqueous solutions by nano-polypropylene-titanium dioxide: optimization of adsorption based on response surface methodology (RSM) and central composite design (CCD), Korean J. Chem. Eng., 38 (2021) 2436–2445.
[23] H. Karyab, F. Karyab, R. Haji-Mirmohammad Ali, Optimization of adsorption conditions for removal of total organic carbon from drinking water using polypropylene and titanium dioxide nano-composite by response surface methodology, Desal. Water Treat., 98 (2017) 144–151.
[24] T.K. Kumaresan, S.A. Masilamani, K. Raman, S. Zh. Karazhanov, R. Subashchandrabose, Dicyandiamide-formaldehyde and Borassus Flabellifer inflorescence assisted preparation of low surface area nitrogen-doped carbon as high-performance anode for lithium-ion batteries, Mater. Lett., 276 (2020) 128218, doi: 10.1016/j.matlet.2020.128218.
[25] L. Gao, L. Xuechuan, H. Song, C. Zhang, T. Wang, X. Gao, Synthesis and decolorization performance of modified dicyan-diamide-formaldehyde decolorant, J. Liaoning Univ. Pet. Chem. Technol., 41 (2021) 23–27.
[26] V. Saritha, N. Srinivas, N.V. Srikanth Vuppala, Analysis and optimization of coagulation and flocculation process, Appl. Water Sci., 7 (2017) 451–460.
[27] S. Papic, N. Koprivanac, A. Metes, Optimizing polymer-induced flocculation process to remove reactive dyes from wastewater, Environ. Technol., 21 (2000) 97–105.
[28] G. Miner, Standard methods for the examination of wat(er) and wastewater, J. Am. Water Works Assn., 98 (2006) 130.
[29] M.A. Bezerra, R.E. Santelli, E.P. Oliveira, L.S. Villar, L.A. Escaleira, Response surface methodology (RSM) as a tool for optimization in analytical chemistry, Talanta, 76 (2008) 965–977.
[30] S. Bhattacharya, Central Composite Design for Response Surface Methodology and Its Application in Pharmacy, P. Kayaroganam, Ed., Response Surface Methodology in Engineering Science, InTechOpen, 2021.
[31] S.A. El-Mekkawi, R.A. Abdelghaffar, F. Abdelghaffar, S.A. El-Enin, Application of response surface methodology for color removing from dyeing effluent using de-oiled activated algal biomass, Bull. Natl. Res. Cent., 45 (2021) 80, doi: 10.1186/s42269-021-00542-w.
[32] M. Gholami, Z. Mosakhani, A. Barazandeh, H. Karyab, Adsorption of organophosphorus malathion pesticide from aqueous solutions using nano-polypropylene-titanium dioxide composite: equilibrium, kinetics and optimization studies, J. Environ. Health Sci. Eng., 21 (2023) 35–45.
[33] A. Barazandeh, H.A. Jamali, H. Karyab, Equilibrium and kinetic study of adsorption of diazinon from aqueous solutions by nano-polypropylene-titanium dioxide: optimization of adsorption based on response surface methodology (RSM) and central composite design (CCD), Korean J. Chem. Eng., 38 (2021) 2436–2445.
[34] M. Sarabadan, H. Bashiri, S.M. Mousavi, Removal of crystal violet dye by an efficient and low-cost adsorbent: modeling, kinetic, equilibrium and thermodynamic studies, Korean J. Chem. Eng., 36 (2019) 1575–1586.
[35] M. Wang, Y. Tian, X. Zhao. X. Li, The application of an efficient modified decolorizer in coagulation treatment of high color reclaimed water, Water Sci. Technol., 77 (2018) 2190–2203.
[36] R. Atakan, A. Bical, E. Celebi, G. Ozcan, N. Soydan, A.S. Sarac, Development of a flame-retardant chemical for finishing of

cotton, polyester, and CO/PET blends, J. Ind. Text., 49 (2019) 141–161.
[37] M. Khosravi, S. Arabi, Application of response surface methodology (RSM) for the removal of methylene blue dye from water by nano zero-valent iron (NZVI), Water Sci. Technol., 74 (2016) 343–352.
[38] Z. Yang, X. Lu, B. Gao, Y. Wang, Q. Yue, T. Chen, Fabrication and characterization of poly (ferric chloride)-polyamine flocculant and its application to the decolorization of reactive dyes, J. Mater. Sci., 49 (2014) 4962–4972.
[39] T.Z. Mahmoudabadi, P. Talebi, M. Jalili, Removing Disperse red 60 and Reactive blue 19 dyes removal by using *Alcea rosea* root mucilage as a natural coagulant, AMB Express, 9 (2019) 113, doi: 10.1186/s13568-019-0839-9.
[40] M.J. Puchana-Rosero, E.C. Lima, B. Mella, D. da Costa, E. Poll, M. Gutterres, A coagulation–flocculation process combined with adsorption using activated carbon obtained from sludge for dye removal from tannery wastewater, J. Chil. Chem. Soc., 63 (2018) 3867–3874.
[41] N. Sakkayawong, P. Thiravetyan, W. Nakbanpote, Adsorption mechanism of synthetic reactive dye wastewater by chitosan, J. Colloid Interface Sci., 286 (2005) 36–42.
[42] Y.M. Slokar, A.M. Le Marechal, Methods of decoloration of textile wastewaters, Dyes Pigm., 37 (1998) 335–356.
[43] X. Jiang, K. Cai, J. Zhang, Y. Shen, S. Wang, X. Tian, Synthesis of a novel water-soluble chitosan derivative for flocculated decolorization, J. Hazard. Mater., 185 (2011) 1482–1488.
[44] A. Assadi, A. Soudavari, M. Mohammadian, Comparison of electrocoagulation and chemical coagulation processes in removing Reactive red 196 from aqueous solution, J. Human Environ. Health Promot., 1 (2016) 172–182.
[45] S.S. Moghaddam, M.A. Moghaddam, M. Arami, Coagulation/flocculation process for dye removal using sludge from water treatment plant: optimization through response surface methodology, J. Hazard. Mater., 175 (2010) 651–657.
[46] M.A. Al-Ghouti, D.A. Da'ana, Guidelines for the use and interpretation of adsorption isotherm models: a review, J. Hazard. Mater., 393 (2020) 122383, doi: 10.1016/j.jhazmat.2020.122383.
[47] J. Wang, X. Guo, Adsorption isotherm models: Classification, physical meaning, application and solving method, Chemosphere, 258 (2020) 127279, doi: 10.1016/j.chemosphere.2020.127279.
[48] M.M. Majd, V. Kordzadeh-Kermani, V. Ghalandari, A. Askari, M. Sillanpää, Adsorption isotherm models: a comprehensive and systematic review (2010–2020), Sci. Total Environ., 812 (2022) 151334, doi: 10.1016/j.scitotenv.2021.151334.
[49] J. Wang, X. Guo, Adsorption kinetic models: physical meanings, applications, and solving methods, J. Hazard. Mater., 390 (2020) 122156, doi: 10.1016/j.jhazmat.2020.122156.
[50] F.-C. Wu, R.-L. Tseng, S.-C. Huang, R.-S. Juang, Characteristics of pseudo-second-order kinetic model for liquid-phase adsorption: a mini-review, Chem. Eng. J., 151 (2009) 1–9.
[51] S.K. Milonjić, A consideration of the correct calculation of thermodynamic parameters of adsorption, J. Serb. Chem. Soc., 72 (2007) 1363–1367.
[52] A. Myers, Thermodynamics of adsorption in porous materials, AlChE J., 48 (2002) 145–160.